Mitigation of ice loading

Feasibility study of a semi-active solution

Arkadiusz Mroz
VTT Building and Transport
IPPT – Institute of Fundamental Technological Research, Warsaw, Poland

Tuomo Kärnä
VTT Building and Transport

ISBN 951–38–6591–6 (URL: http://www.vtt.fi/inf/pdf/)
ISSN 1459–7683 (URL: http://www.vtt.fi/inf/pdf/)

JULKAISIJA – UTGIVARE – PUBLISHER

VTT, Vuorimiehentie 5, PL 2000, 02044 VTT
puh. vaihde 020 722 111, faksi 020 722 4374

VTT, Bergsmansvägen 5, PB 2000, 02044 VTT
tel. växel 020 722 111, fax 020 722 4374

VTT Technical Research Centre of Finland, Vuorimiehentie 5, P.O.Box 2000, FI–02044 VTT, Finland
phone internat. +358 20 722 111, fax +358 20 722 4374

VTT Rakennus- ja yhdyskuntatekniikka, Kemistintie 3, PL 1805, 02044 VTT
puh. vaihde 020 722 111, faksi 020 722 7007

VTT Bygg och transport, Kemistvägen 3, PB 1805, 02044 VTT
tel. växel 020 722 111, fax 020 722 7007

VTT Building and Transport, Kemistintie 3, P.O.Box 1805, FI–02044 VTT, Finland
phone internat. +358 20 722 111, fax +358 20 722 7007

Technical editing Anni Kääriäinen

Published by

Series title, number and
report code of publication

VTT Working Papers 39
VTT–WORK–39

Author(s)
Mroz, Arkadiusz & Kärnä, Tuomo

Title

Mitigation of ice loading
Feasibility study of semi-active solution

Abstract

Conical structures are commonly used in order to mitigate the ice loading on off shore structures. However a need for further mitigation of the structure response is recognised. This report introduces a new, semi-active solution aiming at mitigation of ice forces acting on off shore towers. New interface between the cone and tower is introduced. So-far-used rigid connection is replaced with compliant connection using adaptive springs and dampers. Adaptation procedure is introduced in order to optimise the effect. The solution aims at decreasing of the horizontal component of ice loading and does not affect the period of excitation. The feasibility study of new solution effectiveness is performed. Simulations are done using ABAQUS/Standard software.

Keywords
ice loading, conical structures, semi-active control, off-shore structures, simulation, wind turbine structures, towers, cone structure, vibrations, fatique control

Activity unit
VTT Building and Transport, Kemistintie 3, P.O.Box 1805, FI–02044 VTT, Finland

ISBN		Project number
951–38–6591–6 (URL: http://www.vtt.fi/inf/pdf/)		R3SU00222
Date October 2005	Language English	Pages 34 p.
Name of project Sulautettu rakenneäly	Commissioned by VTT	
Series title and ISSN VTT Working Papers 1459–7683 (URL: http://www.vtt.fi/inf/pdf/)	Publisher VTT Information Service P.O. Box 2000, FI–02044 VTT, Finland Phone internat. +358 20 722 4404 Fax +358 20 722 4374	

Contents

List of symbols

RF1, R_H – horizontal reaction force

RF2, R_V – vertical reaction force

x_d – cone top edge horizontal displacement

α – inclination angle of the cone

D – waterline diameter of the cone

H – cone height

σ_{11} – compressive stress in ice, at the cone – ice-sheet contact point, direction 1

σ_{22} – tensile stress in ice, at the cone – ice-sheet contact point, direction 2

ξ_i – structural damping coefficient

L_b – breaking length of ice

v – ice flow velocity

μ – friction coefficient between ice sheet and cone

h – ice sheet thickness

k – spring stiffness

c – damping coefficient

1. Introduction

VTT is currently making concentrated research efforts within a Technology Theme *Intelligent Products and Systems* with a focus area *Embedded Structural Intelligence*. This piece of research work was carried out within a sub-project entitled *Intelligent Wind Turbines* (SULAWIND).

The use of wind power has doubled every 2–4 years worldwide. One key element enabling the growth in market is the improved efficiency and economics of wind technology reached through the further increased size of wind turbines. Along with the growth of the size, the slenderness of wind turbines has increased leading to increased importance of vibration and fatigue control of all components of the structures. The operating environment of large offshore wind turbines is more hostile and complex compared to that of today's onshore wind turbines. The turbines are exposed to severe climatic conditions. The turbines must be designed to operate with less maintenance.

Intelligent materials and systems have been developed for the aviation industries, machine industries and for the mitigation of damages due to earthquakes. VTT has been active in these areas. Both the growth in size and the increasing requirements call for more adaptive solutions to be used. Successful use of these solutions would contribute to larger step-changes in the development of wind technology.

The preceding research efforts within the project Embedded Structural Intelligence include developments of smart devices that are based on either on MR elastomers or on a special solution to control the stiffness of a uniaxial load carrying element. In the present report, we presume that such smart devises have been fully developed and study how they can be efficiently used in an offshore wind turbine structure to mitigate vibrations.

A traditional approach to mitigate vibrations is to promote the energy dissipation within the structure. Kärnä and Kolari (2004) studied this option in the case of a narrow-band random excitation caused by sea ice. They found that the maximum dynamic response can be reduced by a factor of 2 to 2.5 if a passive tuned mass damper (TMD) or a tuned liquid damper (TLD) is installed on top of the wind turbine tower. The performance can be increased by about 25% if the passive damper is modified into a semi-active one. These results were not encouraging. Therefore another basic approach was adopted for this work. In ice-infested sea areas, the moving sea ice can cause structural vibrations. A method will be studied to reduce the dynamic effects already at the point of the ice action.

2. The idea of "Smart Cone"

The past experience in ice engineering shows that dynamic problems are likely to arise on an offshore structure that is compliant and has a relatively narrow and vertical face against the ice. Very severe self-induced vibrations have been encountered in such conditions. To prevent this situation, it has become customary to fix an additional cone-shaped component on the foundation. This solution usually reduces both static and dynamic ice actions. However, the full-scale measurements conducted in the Bohai Bay (Yue & Bi, 2000; Qu et al., 2003; Li et al., 2003) show that transient or narrow-band random vibrations can still remain as a problem for the structure.

Instead of using a fixed cone, Lindqvist and Juurmaa (1982) proposed the use of a compliant cone that can move in vertical direction relative to the shaft of the main structure. Correspondingly, Wang (2005) studied a compliant solution where the cone is separated from the main structure by horizontal springs. A third option of using compliant cones will be studied herein.

Cone – shaped structures installed on off-shore towers subjected to ice loading aim at inducing bending failure of the ice sheet. Since the total interaction force acts normal to the structure's surface, the slope of a cone introduces the vertical component of the loading. As the ice sheet comes to the contact with cone, both horizontal and vertical components increase; the horizontal component, which causes the tower vibration, produces compression (eventually may cause crushing), and the vertical component produces bending in the deforming ice sheet. When the value of the vertical force achieves a certain level, the ice sheet fails by bending. Compared to the case without a cone, the maximum horizontal force, corresponding to the instance of ice failure, is decreased substantially.

The idea of the "Smart Cone" is to further decrease the horizontal reaction acting on the tower and inducing vibrations, without changing the vertical component responsible for the bending failure of ice. This could be achieved by introducing new cone – tower interface as shown on Figure 1.

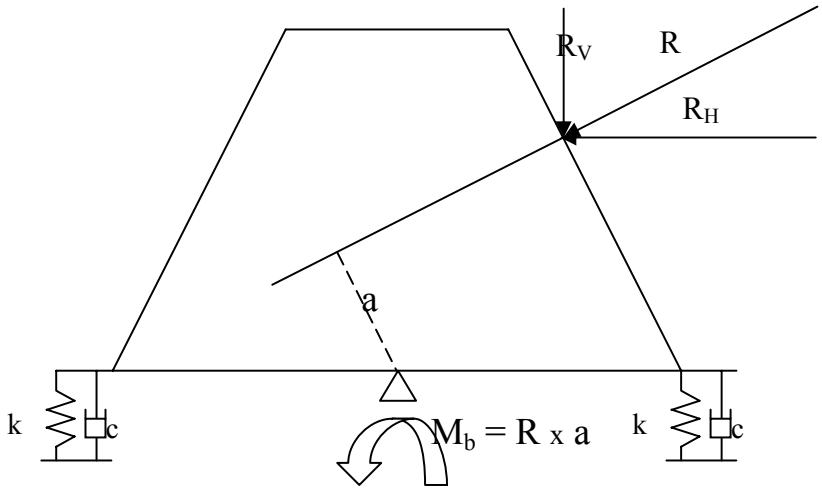

Figure 1. New cone – tower interface.

Once at the contact with ice the cone will rotate together with the ice sheet. Because the cone is now free to move together with the pressing ice, the ice compression (crushing) is limited, and so is the horizontal reaction. On the other hand the bending of the ice sheet is preserved allowing for the bending failure. Configuration at the instant of ice breaking is shown on Figure 2.

Semi-active control of the spring and dashpot coefficients is required in order for the solution to be efficient – on one hand, and for the cone to return to its initial position before next peak – on the other.

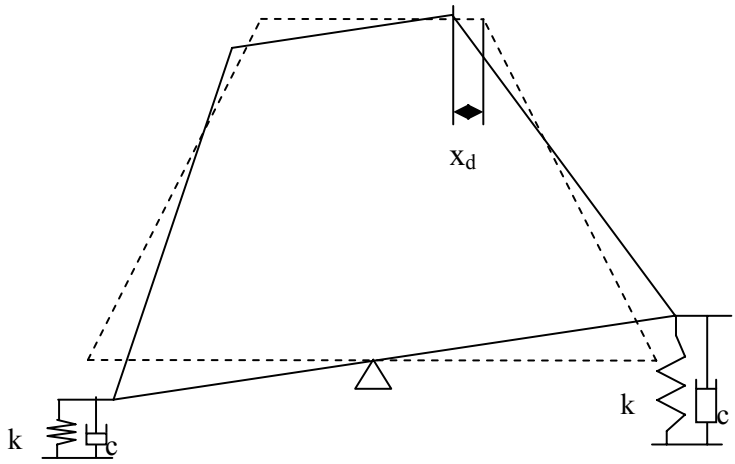

Figure 2. Configuration at the instant of ice breaking.

3. Simulations – introduction

In order to prove the effectiveness of the new solution one would be tempted to carry out the complete dynamic simulation of ice-cone-tower interactions where the periodical ice loading is modelled by the contact forces between ice and cone. This would, however, involve a mechanical model of ice material capable of simulating cracks and bending and crushing failures in order to represent the sequence of contact or failure phases. Development of such material model could be a challenge for another study. For our purposes the task has been split into two simulations:

I) Static analysis of the cone-ice interaction in order to obtain the maximum static reaction forces acting on tower. The aim of this simulation is to compare the reactions generated for the new solution with the reference case, for the same value of displacement prescribed to the ice sheet.

II) Dynamic analysis of the wind turbine structure. Static forces are used to generate the periodic loading pattern applied to the structure. The aim of this simulation is to discuss the effectiveness of the new solution in terms of tip of the tower and tip of the blade displacements. Furthermore the inertia effect of swinging cone on the behaviour of tower is analysed.

4. Simulation of the cone – ice interaction

4.1 FEM model in ABAQUS/Standard

The general set-up for the simulation is shown on Figure 3.

Some of the main features of the model are discussed below.

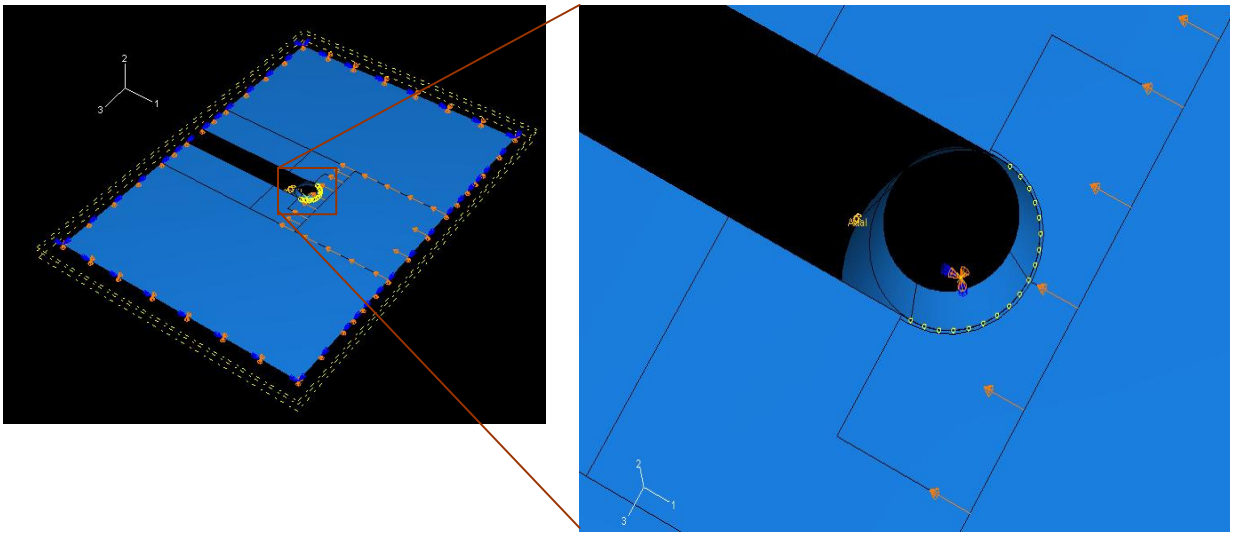

Figure 3. Cone – ice interaction ABAQUS model overview.

The ice field was modelled with S4R shell elements with finite membrane strains and the cone was modelled with discrete rigid body elements R3D4.

The geometry of the cone is shown on Figure 4.

Cone rigid body was fixed at its reference point except for the d.o.f. no. 6 (Ralston, 1977) which was set free. This rotation was then controlled by two Axial Connector elements. Elasticity and damping behaviour was defined for these connectors. Note, that the velocities can be calculated in the static analysis, and so can be the viscous force. The damping coefficient c = 4000 N/(m/s) was assumed, and the spring stiffness k = 50 ÷ 500 kN/m (various cases were considered).

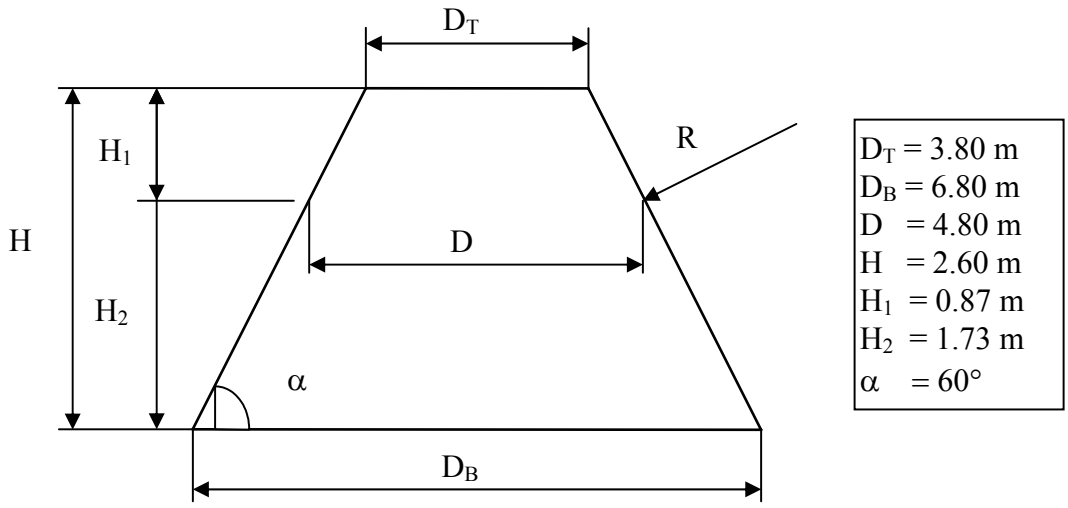

Figure 4. Cone dimensions.

A total displacement of 5 cm was prescribed to a region of the ice field. Boundary conditions for the ice field were applied relatively far from the cone – ice contact area.

A node – region contact area was defined for the cone – ice interaction, with the cone acting as a master surface and part of the ice boundary acting as a slave surface. Initial align option was used to make sure that the slave nodes are initially in contact with the master surface. Tangential behaviour of the contact was defined as Penalty type frictional contact with the friction coefficient $\mu = 0.15$.

The material model for the ice sheet was chosen as elastic – perfectly plastic material with Young Modulus E = 4.0 GPa, and the yield stress σ_{pl} = 0.7 MPa. Because the model of ice is very simplified we do not expect to obtain reactions which correspond to the failure point of the ice. Without knowing the actual point at which the ice fails and thus, at which we should read the reactions – we can only see how the reactions increase as the total displacement is gradually applied. We can also compare the results with reference case of fixed cone – and in this way judge the effectiveness of our solution.

The total displacement (0.05 m) will be applied gradually in 200 increments over the time period of 0.05 sec. This corresponds to the velocity of the ice field flow of 1.0 m/s. A single General Static step was created to perform the analysis.

For the reference case the same model was used, except the cone was fixed at its reference point at all 6 degrees of freedom and consequently no connectors were used.

4.2 Results of simulation

4.2.1 Table of results

The results of simulations are discussed in terms of (Figure 5)

a) reaction forces at the cone reference point
b) stresses in ice at the point where the initial crack should occur
c) horizontal displacement of the top edge of the cone.

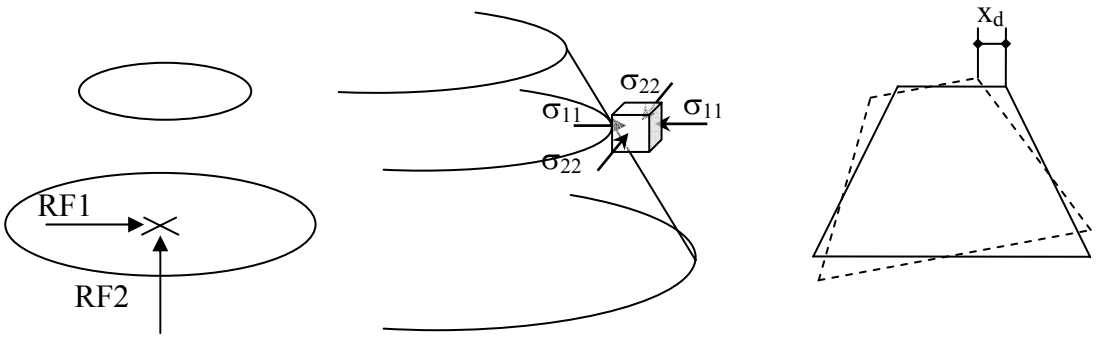

Figure 5. Chosen results quantities.

Table 1. Simulation results.

Description	Parameters		RF1 [kN]	RF2 [kN]	σ_{11} [kPa] *	σ_{22} [kPa] *	x_d [cm]
	Spring stiff. k [N/m]	Ice thick. t [m]					
Reference case, cone fixed	–	0.50	322.8	128.1	–458.7	152.7	–
New solution	50 000	0.50	190.2	111.4	–213.2	422.6	7.05
New solution	100 000	0.50	206.6	111.6	–240.2	399.6	6.91
New solution	250 000	0.50	252.0	111.8	–316.3	331.1	6.50
New solution	500 000	0.50	278.9	116.3	–368.7	268.7	4.59
Reference case, cone fixed	–	0.75	890.7	360.1	–506.2	231.0	–
New solution	50 000	0.75	463.6	324.9	–238.5	490.1	7.50
New solution	100 000	0.75	481.6	325.3	–250.3	483.3	7.43
New solution	250 000	0.75	533.6	325.9	–289.2	454.0	7.26
New solution	500 000	0.75	615.1	326.2	–347.9	408.9	7.01

* (+) – tension, (-) - compression

4.2.2 Discussion of reaction forces

For both considered ice thickness' the best results were obtained for the lowest possible spring stiffness. The reason, parameter k cannot be further decreased is that the cone will have to return to its initial position after the ice fails. If there was no spring stiffness at all, than the effect in decreasing the RF1 would be the most significant, but the device could not work in a repetitive sequence. It can be seen from Table 1 that for k = 50 kN/m there is still 41% and 48% mitigation of the horizontal component for ice thickness 50 cm and 75 cm, respectively. For spring stiffness k = 500 kN/m the solution effectiveness drops to 14% and 31% respectively. The vertical component of reaction force is not affected significantly by the new solution. Values of RF2 are decreased only by 13% and 10% for both cases. In practice the vertical component could be preserved in order to impose ice sheet bending.

The dependency of the horizontal reaction reduction on the spring stiffness is shown on Figure 6.

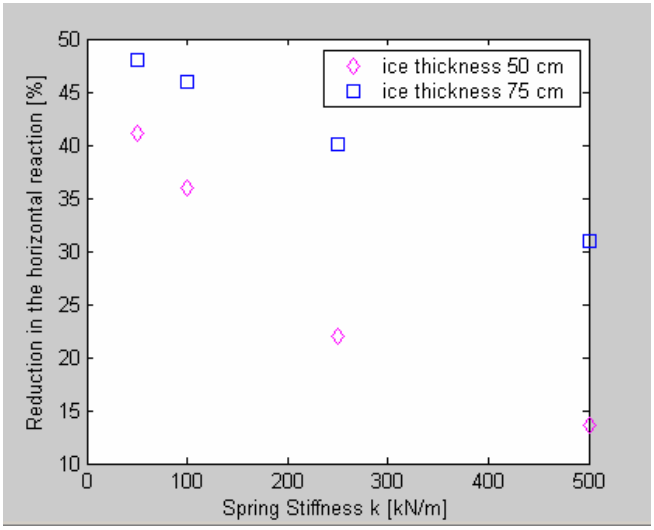

Figure 6. Change in horizontal reaction as function of spring stiffness.

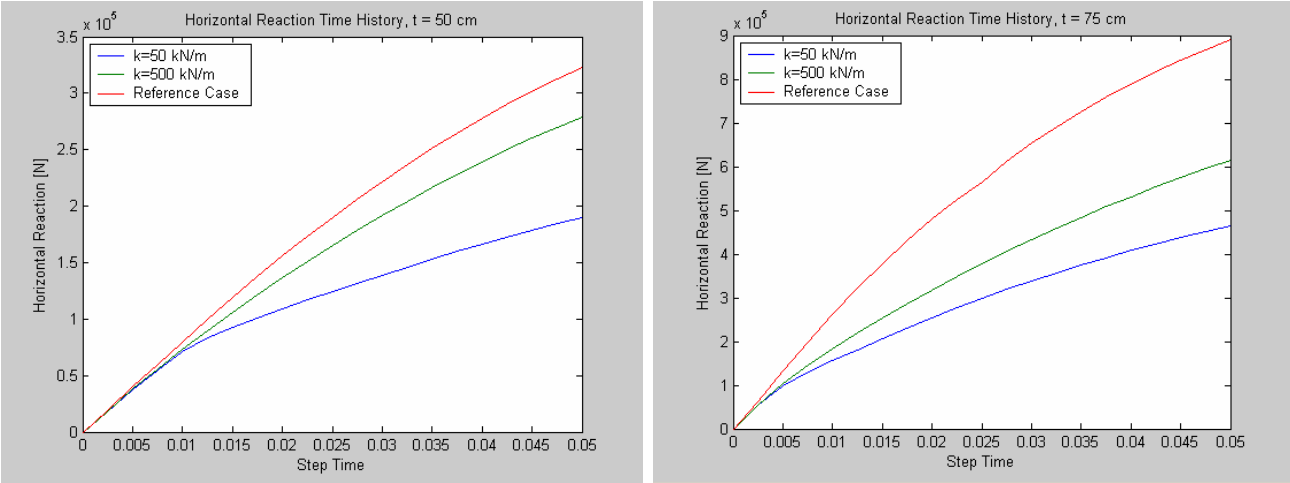

Figure 7. Time history of the horizontal reaction change.

Figure 7 represents the Time History data showing the reaction increase due to the increase in prescribed displacement. The first yielding occurs between 0.005 and 0.01 sec. resulting in non-linear growth of the reactions in the remaining time period.

4.2.3 Discussion of stresses in the ice sheet

It can also be seen that the stresses σ_{11} which are effect of the ice pressing against the cone and thus produce the horizontal reaction force on the tower are decreased by 54% and 53% for considered ice thickness'. On the other hand the stresses σ_{22} which are tensile and would produce the initial radial crack are increased by 177% and 112% respectively. In practice the new solution could produce a clearer bending mode failure in the ice sheet.

Figure 8 shows a typical map of Mises stress with the yield area, and Figure 9 shows vertical displacement of the ice sheet and cone.

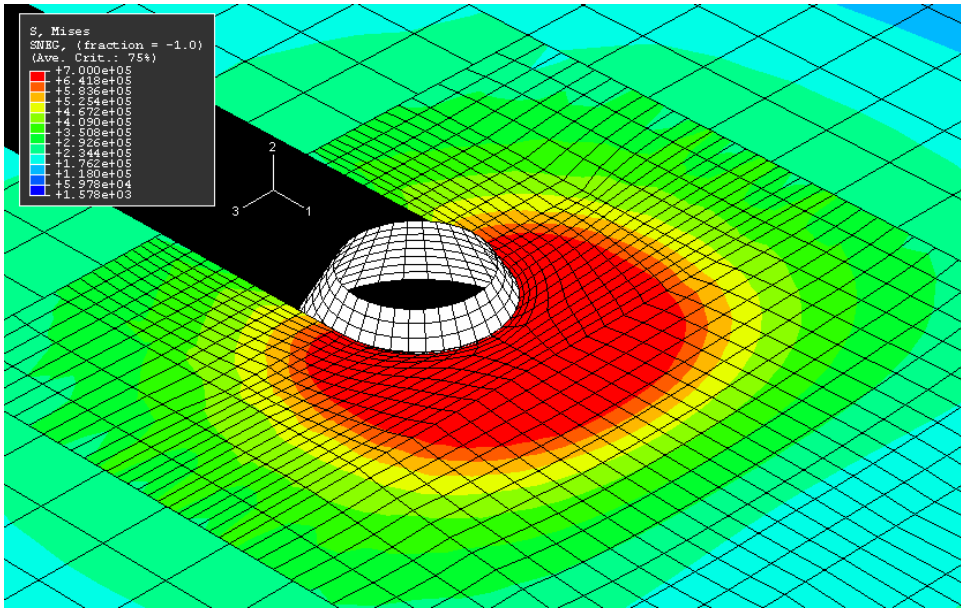

Figure 8. Map of Mises stress in the ice sheet.

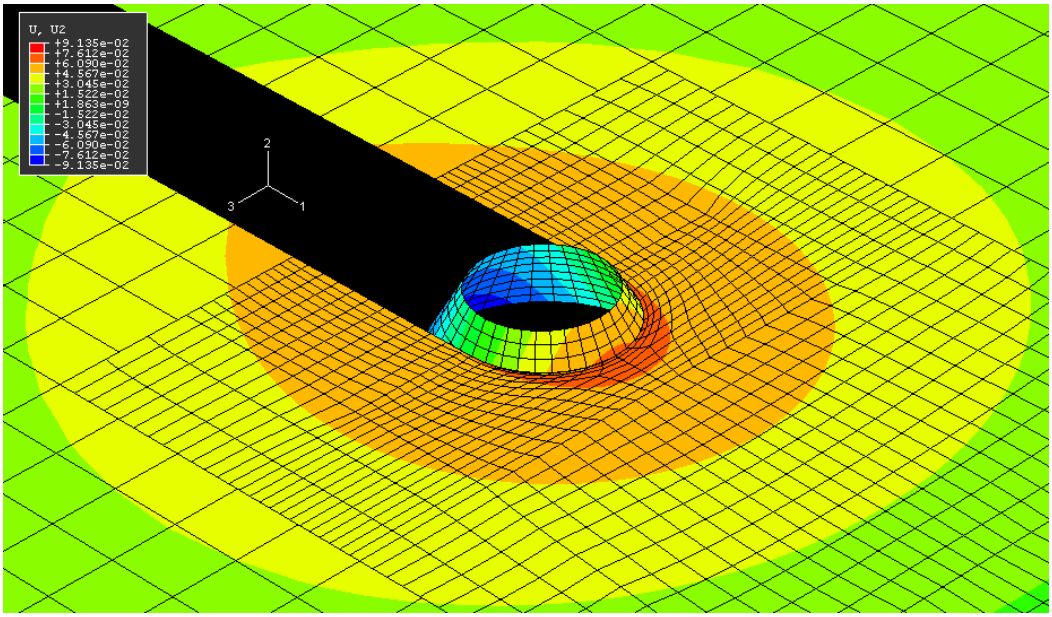

Figure 9. Vertical displacements of ice sheet and cone.

4.2.4 Other considerations

In the initial configuration there is a full geometry compliance between the master surface and the slave nodes therefore analysis begins with the full contact. However, the deformation of the system makes adjacent geometries non-compliant and thus the contact is preserved only on less than 30% of the initial contact length. In practice the contact length would be bigger since the ice near the cone is locally weaken or damaged

and thus better adjusts to the cone geometry. This phenomenon is not taken into account here. The contact length would also change depending if the ice is strong or soft.

Furthermore a decrease in the spring stiffness does not cause a significant increase in deflection of the cone, because the rotation of the cone is constrained not only by springs but also by the ice sheet itself. Figure 10 illustrates the final configuration of cone and the bending of ice sheet (connector elements not displayed).

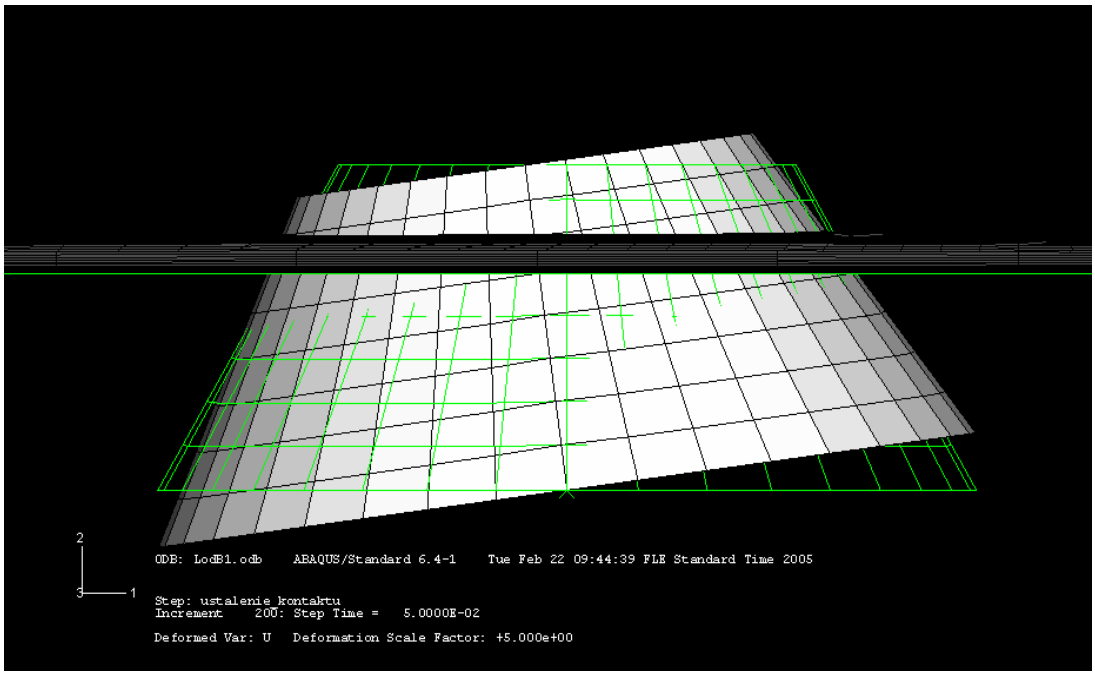

Figure 10. Deformed model.

4.2.5 Conclusion

The simulation shows that proposed solution could reduce the horizontal reaction by 41% and 48% for considered ice thickness given that the spring and dashpot coefficients are possibly small allowing for the cone rotation.

The change in the values of stresses indicates that the new solution could produce a clearer bending failure in the ice sheet.

A second simulation is needed in order to investigate the effectiveness of new solution in terms of tower and blades displacements. It will also show the dynamic behaviour of cone under periodic loading and – if needed – allow us to develop a control algorithm for the spring and dashpot coefficients which would optimise the cone behaviour. Also the effect of inertia of the moving cone on the tower will be analysed.

5. Dynamic analysis of the wind turbine structure

5.1 Dynamic model of a wind turbine tower

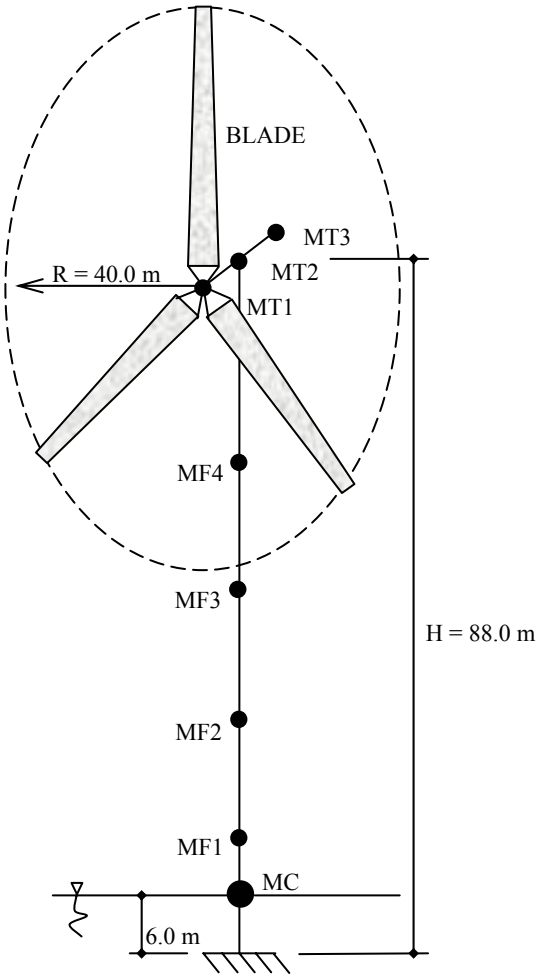

- ✓ **Blade** (S4R5 shell elements):
  Material properties and shell thickness were chosen so that the first own frequency and weight of blade are $\omega_1 = 1.30$ Hz, G = 7006 kg

- ✓ **Tower** (B33 beam elements):
  47 elements with circular section were used, radius R = 1.161 ÷ 2.111 m, thickness t = 0.014 ÷ 0.040 m.
  Weight of tower $G_T = 186\ 782$ kg

- ✓ **Point masses** (MASS elements):
  MT1 = 13 000 kg
  MT2 = 31 800 kg turbine
  MT3 = 35 000 kg
  MF1 = 4 200 kg
  MF2 = 3 200 kg flanges
  MF3 = 1 900 kg
  MF4 = 2 300 kg
  MC = 49 620 kg - cone + water

Figure 11. Dynamic model of the wind turbine tower.

The main features of the wind turbine structure model are shown on Fig. 11. Mass Elements and blades were connected to the tower with rigid connector elements in order to obtain a realistic mass distribution in space. The additional water mass effect is included and will be discussed later.

The total weight of the structure is

186 782 + 3 x 7006 + 141 020 = 348 820 kg.

5.2 Own frequencies extraction

Table 2 lists the first 7 own frequencies of the structure.

Table 2. Own frequencies of the model.

Mode	Frequency [Hz]	Period [sec]
1	0.320	3.125
2	0.322	3.106
3	0.985	1.015
4	1.129	0.886
5	1.293	0.773
6	1.557	0.642
7	2.230	0.448

5.3 Damping

Structural damping was assumed to be 0.5% of the critical damping. Rayleigh mass and stiffness proportional damping coefficients were obtained from equation (1). (ABAQUS, 2004.)

$$\xi_i = \alpha_R/(2 \times \omega_i) + (\beta_R \times \omega_i)/2 \quad (1)$$

ξ_i was assumed 0.5% for $\omega_1 = 0.320$ and $\omega_7 = 2.230$ Hz, which gives damping coefficients of $\alpha_R = 0.0028$ and $\beta_R = 0.0039$.

5.4 Loading

5.4.1 Critical breaking length

In order for the loading frequency to cause a narrow band excitation the breaking length of ice divided by the ice flow velocity must be equal to the first own period of the tower:

$$L_b / v = T. \quad (2)$$

Therefore, assuming the ice flow velocity v = 1.0 m/s:

$L_b = 1/0.320$ [Hz] x 1.0 [m/s] = 3.13 m.

From works by Li and Yue (2002) and Li et al. (2003) it is possible to find out the ice thickness corresponding to this critical breaking length:

$$L_b = k \times \xi^{1/3} \times h \quad (3)$$

For a distributed ice-structure contact, the length or thickness parameter k can be determined from the equation:

$$k^3 + 0.75 \times (b_{cont}/h) \times \tan(\theta/4) \times k^2 - 83.33 \times \xi - 125 \times b_{cont}/h \times \tan(\theta/4) = 0 \quad (4)$$

where

$$\xi = (\sin\alpha + \mu\cos\alpha)/(\cos\alpha - \mu\sin\alpha)$$

$$\tan(\theta/4) = b_{cont}/(D + \mathrm{sqrt}(D^2 - b^2_{cont})).$$

The contact extent of 30% of initial contact obtained in the Simulation I corresponds to the angle $\theta = 54°$ and the contact width b = 2.18 m. Water diameter of cone D = 4.80 m.

For the cone inclination angle $\alpha = 60°$ and friction coefficient $\mu = 0.15$, the horizontal or vertical force ratio is $\xi = 2.5427$.

It follows from the above formulas that the critical breaking length corresponds to the ice thickness of ca. h = 0.50 m.

Results of the Simulation I obtained for the ice thickness of 0.50 m were chosen for the further analysis.

5.4.2 The reference case loading

The loading applied to the reference case is shown on Figure 12.

A rigid and weightless cantilevers were added in order to simulate the actual way of loading.

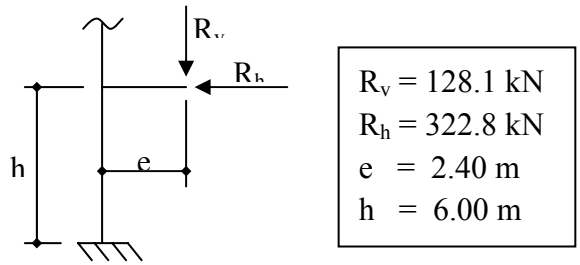

Figure 12. Reference case loading.

For the loading amplitude refer to Figure 14 a).

5.4.3 The new solution loading

The loading applied to the new solution case is shown on Figure 13.

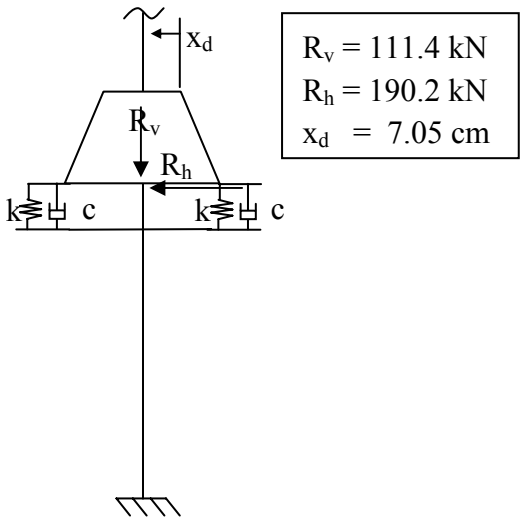

Figure 13. New solution loading.

The reaction forces are applied directly to the tower which corresponds to the reaction forces at the cone reference point in Simulation I.

The spring and dashpot forces as well as inertia forces of the cone will be generated as the prescribed displacement x_d is applied to the cone.

5.4.4 Amplitudes

The peak values shown on Figure 13 are changing throughout the analysis according to amplitudes illustrated on Figure 14. The shape of the forces amplitude was assumed acc. to Qu et al. (2003). Constant values of the peak forces and amplitudes instead of random ones were chosen to have a better view of the solution effectiveness. The period of excitation is 3.13 sec which is equal to the first own period of the tower. The value of forces between the peaks is assumed to be zero, which is a realistic assumption for narrow structures, where almost none of the broken ice stays on the cone. We also assume that the proposed solution will not affect the period of excitation.

The prescribed displacement is ramped from zero to its maximum value and then released so that the cone can swing freely.

An artificial, constant horizontal force of 1.0 kN was added for the purpose of solution convergence. Otherwise the implicit dynamic algorithm had convergence problems in the time intervals where there was no loading.

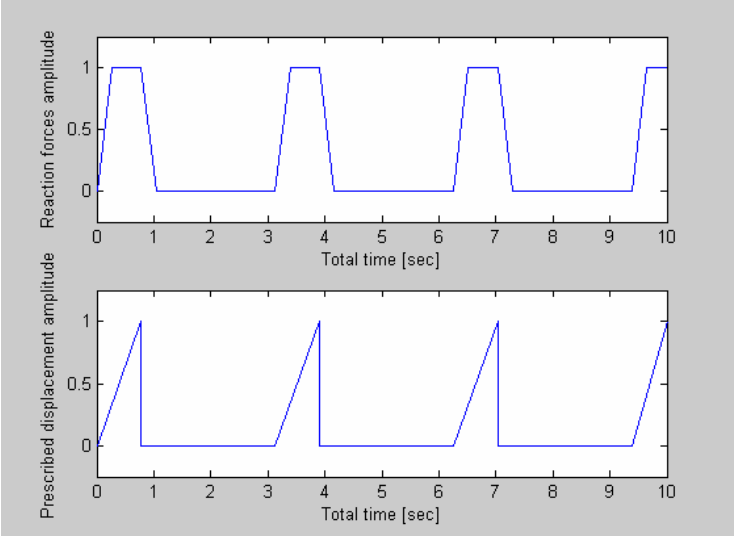

Figure 14. Force and displacement amplitudes.

5.5 The cone

5.5.1 Cone structure

The cone was modelled with S4R shell elements of thickness of 24 cm and density corresponding to the cross section shown on Figure 15.

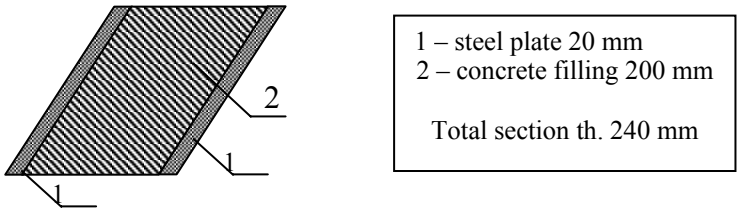

Figure 15. Cone cross section.

$\rho' = 0.17 \times 7850\ kg/m^3 + 0.83 \times 2500\ kg/m^3 = 3410\ kg/m^3$

Given the dimensions shown on Figure 4 the mass of the cone was calculated:

$G = \rho' \times S \times t = 3410\ kg/m^3 \times 49.95\ m^2 \times 0.24\ m = 40\ 879\ kg.$

5.5.2 Additional mass effect

For the submerged part of the cone the additional mass was included in the cone weight equal to the mass of water displaced by the cone. Assuming that the inside of cone is filled with water the volume of water replaced is

$V_w = S_{sb} \times t = 36.44\ m^2 \times 0.24\ m = 8.745\ m^3,$

where S_{sb} is the surface area of the submerged part of cone and t is the cone thickness. Basic dimensions are shown on Figure 4.

$G_w = 1000\ kg/m^3 \times 8.745\ m^3 = 8745\ kg$ (5)

The weight of the submerged part of the cone is $G'_{sb} = 29\ 822$ kg.
Total weight of the underwater part is therefore:
$G_{sb} = 29\ 822\ kg + 8745\ kg = 38\ 567\ kg.$
The density of the underwater part accounting for the added mass of water is
$\rho_{sb}' = 38\ 567\ kg / 8.745\ m^3 = 4408\ kg/m^3.$
The total weight of the cone with additional water mass is
$G_{total} = 40\ 879\ kg + 8745\ kg = 49\ 624\ kg.$

5.5.3 Water damping effect

According to J.F. Wilson (1984) the damping force characterising the fluid – structure interactions can be calculated from the formula

$$F_d = (\hat{c} + C'_d \times \rho \times D/2) \times v \quad (6)$$

where:
$\hat{c}$ – structural damping coeff.,
ρ – fluid density,
D – water diameter of the structure,
$C'_d = C_d \times |u - v|$ – modified drag coefficient in which:
$|u - v|$ – relative velocity between the fluid and structure,
C_d – drag coeff.

Drag coefficient $C_d = 0.6$ basing on the figure 4.6 on page 115 of Wilson (1984), given that the Reynolds number is:

$$Re = (\rho \times u \times D)/\mu = 6.5 \times 10^6 \quad (7)$$

$\rho = 1000$ kg/ m^3	water density
u = 1.0 m/s	fluid flow velocity
D = 5.8 m	averaged diameter of submerged part
$\mu = 0.8909 \times 10^{-3}$ Pa x s	absolute viscosity of water

Assuming that the relative velocity between the fluid and structure is about 0.5 m/s, and taking into account that the structural damping coefficient is already included in the analysis in material properties we can now calculate the water – structure interaction damping coefficient:

$$c' = 0.6 \times 0.5 \text{ m/s} \times 1000 \text{ kg/m}^3 \times 5.8/2 \text{ m} = 870 \text{ [N/(m/s)]/m} \quad (8)$$
$$c = c' \times H_2 = 870 \text{ [N/(m/s)]/m} \times 1.73 \text{ m} = 1505 \text{ N/(m/s)}$$

H_2 is the height of the submerged part according to Figure 4.

5.6 Control

5.6.1 Cone – structure interface

The static model shown on Figure 1 was realised by means of connector elements. Join Type connector elements were used for translation constraints modelling the axis of rotation. Axial Type connector elements with stiffness and damping behaviour were used to model springs and dampers. General view of the cone – structure interface is shown on Figure 16.

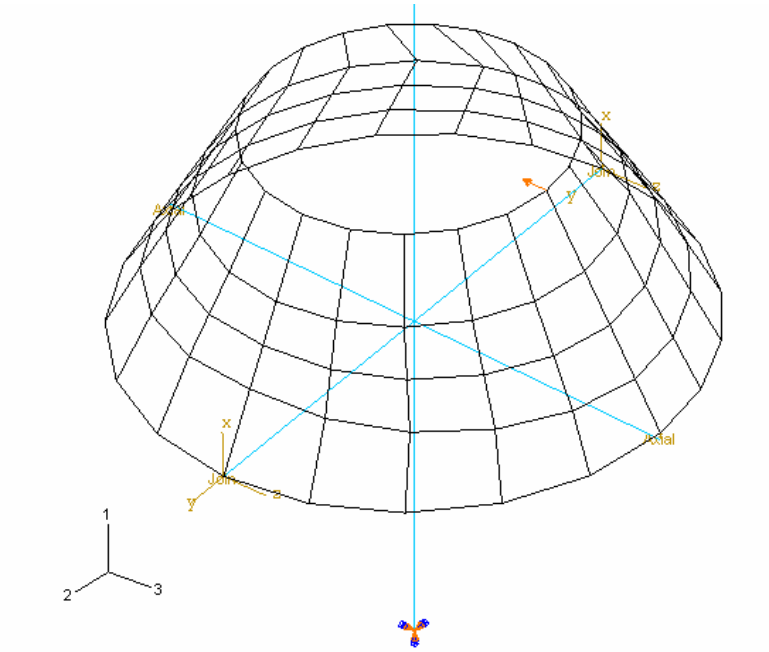

Figure 16. Connector elements joining together cone and tower.

5.6.2 Stiffness and damping control

Various values of spring and dashpot coefficients were considered. The goal was to obtain such values of these parameters that the effectiveness of the solution is high – on one hand, and the cone will come back to its initial position and thus could work in a sequence – on the other. The general conclusion is that for high values of these parameters the cone returns to its initial position before the next peak, but the effectiveness of such solution drops as can be seen on Figure 6. On the other hand for small values the effectiveness is the highest, but the cone movement is not damped out before the next peak. Furthermore the water damping (see p. 5.5.3.) is not enough to damp out cone movement.

Because of the above the only way to achieve the desired effect is to control the stiffness and damping coefficients.

It was assumed that the spring stiffness and the damping coefficient can be adjusted by one order of magnitude. The following procedure controls the real time adaptation of these parameters during the numerical analysis:

1) $k = k_{min}$, $c = c_{min}$
2) if prescribed displacement $x_d = x_{dmax}$ then $k = k_{max}$, $c = c_{max}$
3) if cone edge horizontal velocity v_d = zero then $k = k_{min}$, c – no change
4) if a new peak begins then k – no change, $c = c_{min}$.
5) go to 2).

Up to the point where both the loading and prescribed displacement begin to decrease the parameters have their minimum values, which corresponds to the conditions assumed in Simulation I. Then the parameters are adapted in such a way that at the beginning of the next peak they come back to their initial values.

To include this procedure into the ABAQUS/Standard model two field variables (FV1 and FV2) were introduced at the nodes of Axial Connector elements. FV1 is responsible for adaptation of spring stiffness and FV2 is responsible for adaptation of damping coefficient. Values of these field variables were updated in Fortran procedure UFIELD, depending on the reading from displacement, velocity and load sensors defined and updated in Fortran procedure URDFIL.

Stiffness and damping parameters were adjusted instantly, and their values were as follows:

k_{max} = 500 kN/m k_{min} = 50 kN/m
c_{max} = 40 kN/(m/s) c_{min} = 4 kN/(m/s).

5.6.3 Dependence of axis of rotation on the ice flow direction

In practice the ice field flow changes direction and therefore the structure may come to contact with ice at any point around its circumference. Because of this, it is also a task for the control device to adjust the axis of cone rotation to be always perpendicular to the ice flow direction. This could be realised by means of some structural fuse type of device that either imposes or releases constrains at some point.

This feature is not included in our simulation as we assume that the ice flow direction is perpendicular to the axis of cone rotation.

5.7 Results of simulations

5.7.1 Top of the tower and tip of the blade displacements

Discussed results were obtained from the following input files:

a) *WiatrakB1.inp* – reference case
b) *WiatrakSter3.inp* – new solution.

Deformation of the tower and blades are shown on Figure 17.

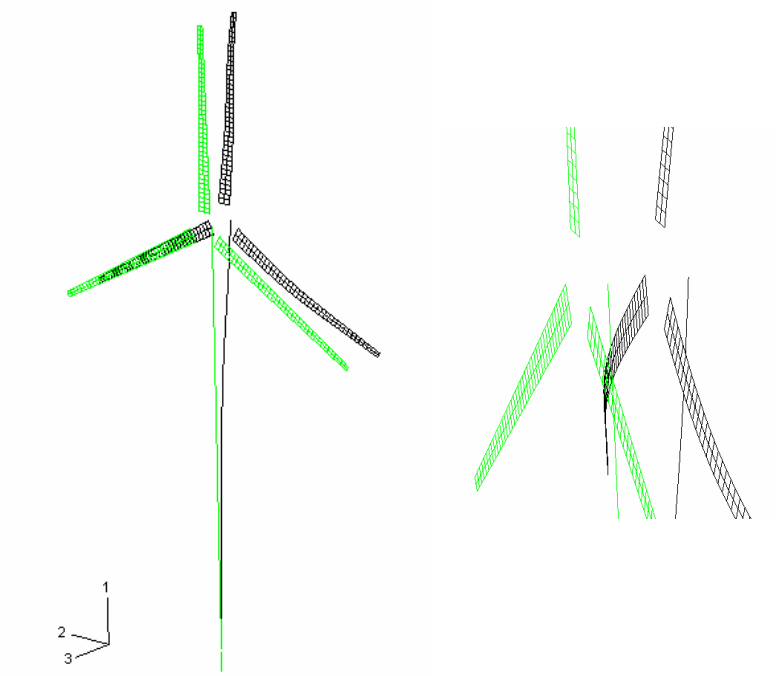

Figure 17. Tower deformation – general view.

Animation of the deformation shows that blades vibrate at higher frequency than the tower as their first own frequency is 1.30 Hz compared to 0.32 Hz in case of tower.

On Figure 18 displacements of the tip of blade and top of tower are compared with the reference case.

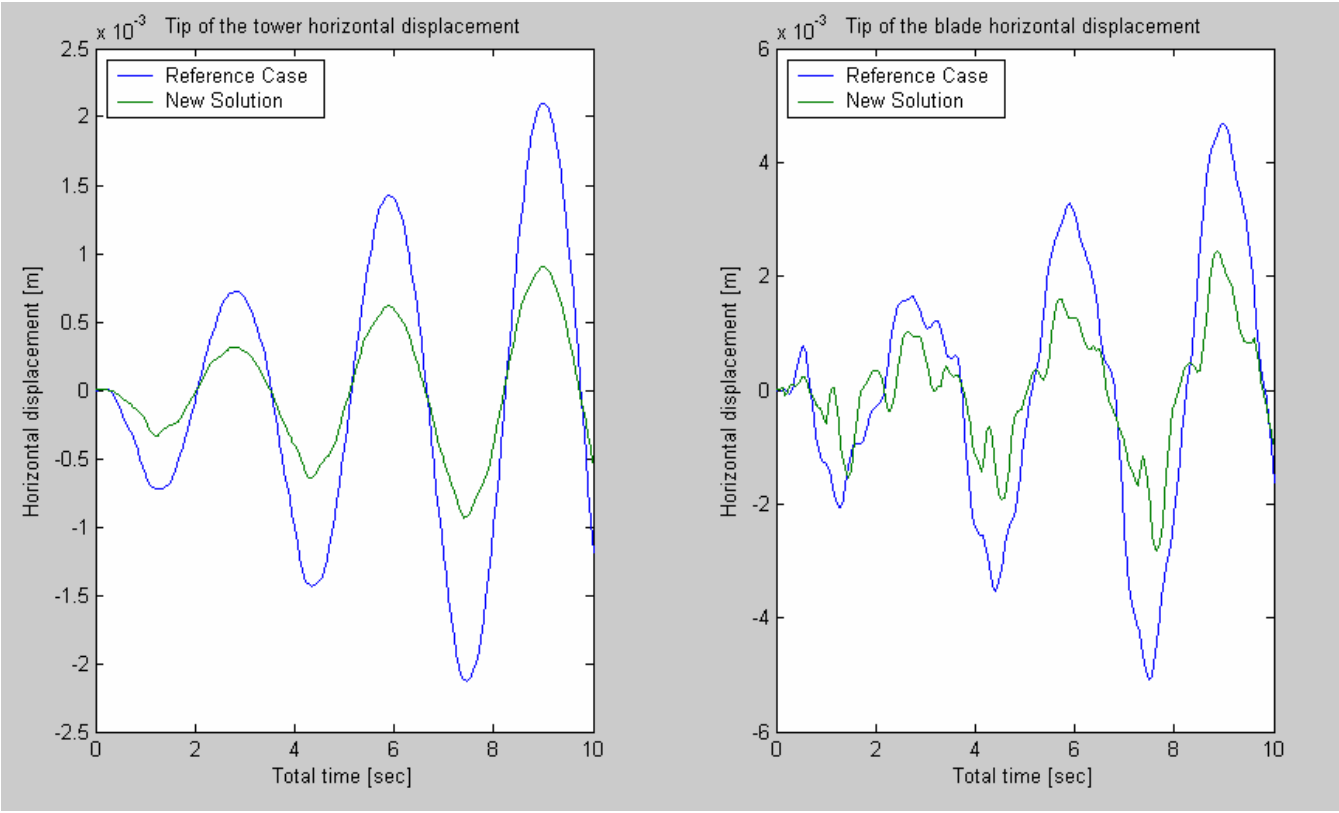

Figure 18. Tower and blade displacement Time History.

The distribution of results in terms of horizontal displacement is shown on Figure 19.

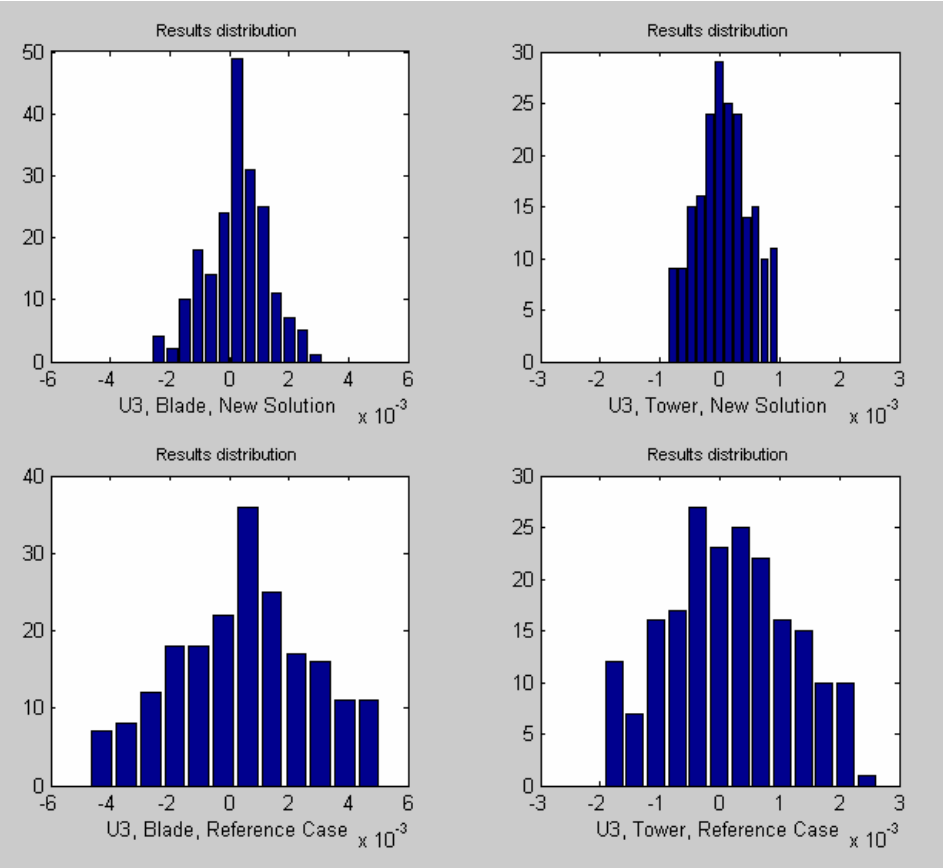

Figure 19. Results distribution.

In Table 3 root mean square values are compared along with maximum and minimum horizontal displacements.

Table 3. Results comparison.

	RMS [m]	U_{max} [m]	U_{min} [m]	Change RMS	Change U_{max}	Change U_{min}
Blade, ref. case	0.00229	0.00469	–0.00510	55%	48%	45%
Blade, new sol.	0.00103	0.00245	–0.00281			
Tower, ref. case	0.00105	0.00210	–0.00213	58%	57%	56%
Tower, new sol.	0.00044	0.00090	–0.00093			

Table 3 shows that 41% decrease in the horizontal reaction correspond to 45% to 48% decrease in the blade response and 55% to 56% decrease in the tower response. RMS values were decreased by 55% and 58% respectively.

58% mitigation of the level of tower vibration can be especially useful from the fatigue strength point of view. Steel wind turbine towers are manufactured of tubular elements connected together on site by flanges. Welds between flanges and steel body plates are subject to high fatigue.

Comparing graph for blade displacements on Figure 18, the influence of the moving cone inertia can be seen. It is described in the point 5.7.2. This effect is considerable and should be taken into account in further analysis.

5.7.2 Cone behaviour

The control scheme described in point 6.6.2 resulted in connector forces illustrated on Figure 20.

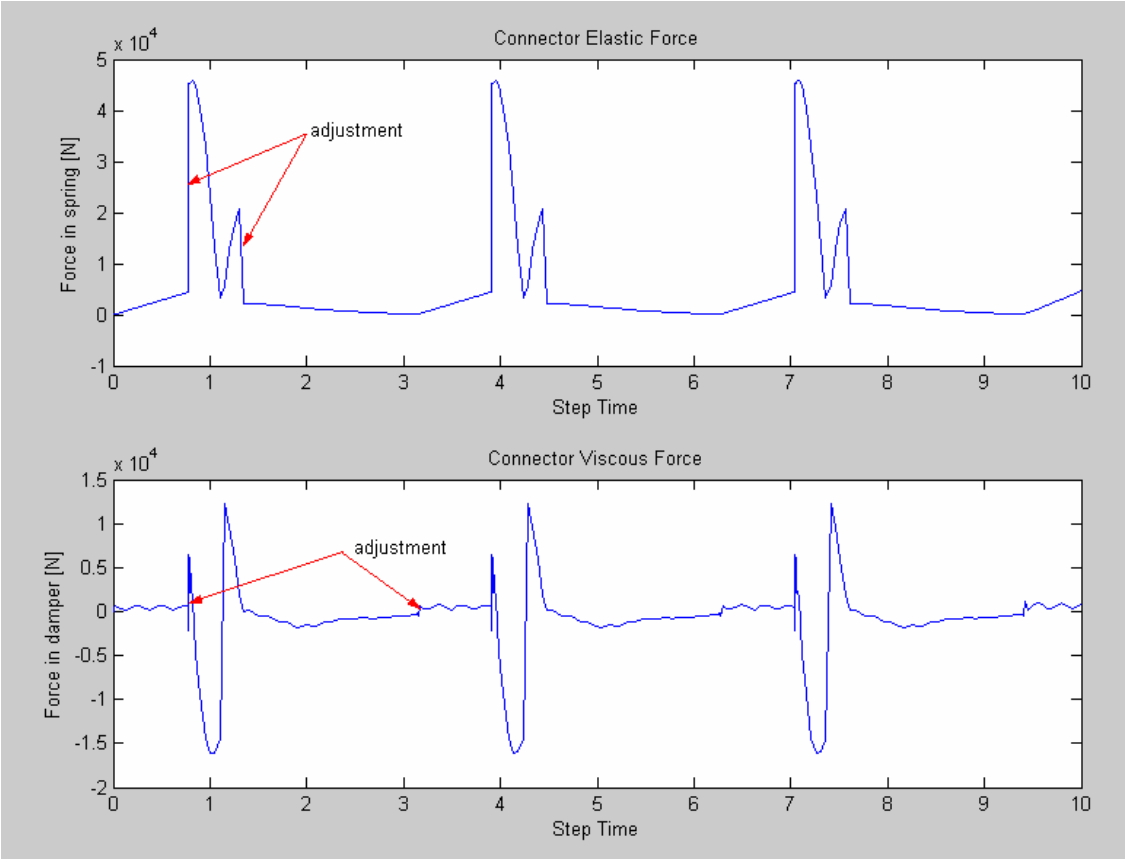

Figure 20. Forces in connector elements.

First adjustment occurs at the same time for spring and dashpot and stands for changing parameters from their minimum to maximum values. The second adjustment occurs at different time instants for spring and dashpot and stands for changing parameters back to their minimum (initial) values.

Time history data for horizontal displacement of the top edge of the cone is shown on Figure 21.

It can be seen that the cone returns to its initial position before the next peak and can work in a repetitive sequence as the ice breaks.

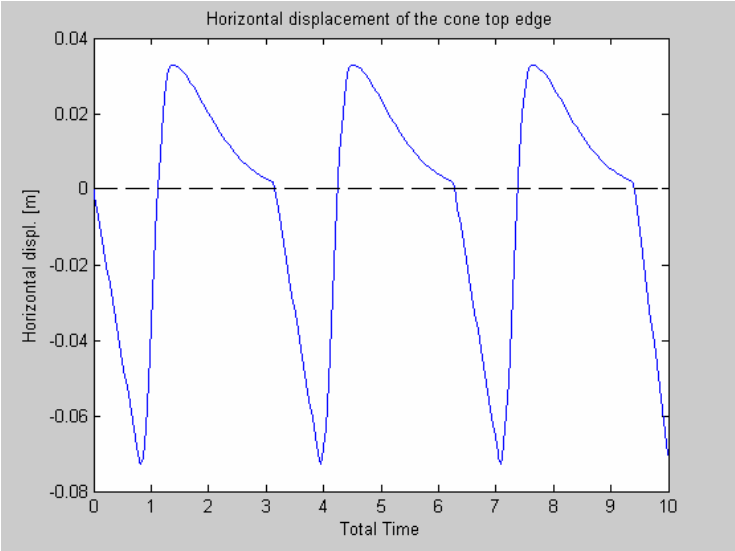

Figure 21. Cone horizontal displacement.

Figure 22 shows the same displacement depicted with the horizontal deflection of the tip of blade. Values of the blade displacements have been magnified 50x. It can be seen that the movement of the cone affects the blade considerably.

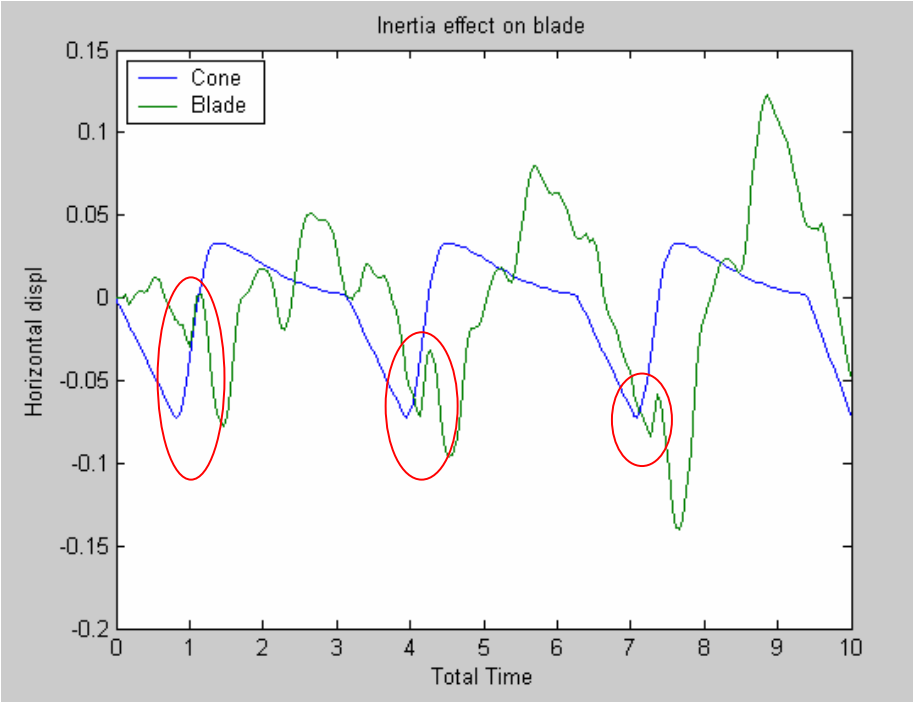

Figure 22. Cone inertia effect in terms of the blade displacement.

The inertia forces of the cone are big enough to influence the behaviour of the blades and thus may help to mitigate their vibrations. This could be the next step of the present study.

6. Summary

This report addresses dynamic problems of offshore structures. In ice-infested sea areas, moving ice sheets can create severe vibrations within the structure. An additional cone that is fixed at the waterline of the structure can be used to reduce both the static and dynamic forces caused by ice. However, full-scale experience shows that this solution does not always completely prevent dynamic ice actions. Transient- and narrow-band random vibrations can remain as a problem.

The performance of the cone can be enhanced by constructing a compliant connection between the cone and the main shaft of the structure. By using a special connection, the incidence angle between the approaching ice sheet and the cone's surface will change while the ice edge is acting and sliding along the cone's surface. This interaction mechanism enhances the bending failure of the ice sheet and, thereby, reduces the horizontal force component. The results obtained herein indicate that an up to 50% decrease in the static and dynamic action effects can be achieved.

The interaction between the ice and structure that is studied here is very complicated. Therefore, some simplifying assumptions were made in the numerical studies. Accordingly, the present report is of a feasibility study and needs further elaborations.

References

ABAQUS Version 6.5. 2004. User's Manual. ABAQUS Inc. Rising Sun Mills, USA. http://www.abaqus.com.

Kärnä, T. & Kolari, K. 2004. *Mitigation of Dynamic Ice Actions on Offshore Wind Turbines.* Proc. 3rd Eur. Conf. On Structural Control, Vienna, Austria.

Li, F. & Yue, Q.J. 2002. *An Analysis for Amplitude and Period of the Alternating Ice Load on Conical Structure.* Proc. 16th Int. Symposium on Ice, Dunedin, New Zealand.

Li, F., Yue, Q.J., Shkhinek, K.N. & Kärnä, T. 2003. *A Qualitative Analysis of Breaking Length of Sheet Ice Against Conical Structures.* Proc. 17th Int. Conf. On Port and Ocean Eng. Under Arctic Conditions, Trondheim, Norway.

Lindqvist, G. & Juurmaa, K. 1982. Suojausmenetelma ja sovitelma (A protection method and its application). Finnish patent application Nr. 822157. Published 28.09.90.

Qu, Y., Yue, Q.J., Bi, X. & Kärnä, T. 2003. *Random Ice Forces on Conical Structures.* Proc. 17th Int. Conf. On Port and Ocean Eng. Under Arctic Conditions, Trondheim, Norway.

Ralston, T.D. 1977. *Ice Force Design Considerations for Conical Offshore Structures*. Proc. 4th Int. Conf. On Port and Ocean Eng. Under Arctic Conditions, Luleå, Sweden.

Wang, L.Y. 2005. The oscillator-indenter for improving ice-induced vibrations. Sixth meeting of the ISO Working Group 8 for Arctic Offshore Structures. December 10–12, 2004. Presentation at the technical workshop of the meeting.

Wilson, J.F. 1984. *Dynamics of Offshore Structures*. New York: Wiley.

Yue, Q.J. & Bi, X.J. 2000. Ice-induced jacket structure vibrations in Bohai Sea. *J. of Cold Regions Engineering [ASCE] 14*(2): pp. 81–92.□4□, pp. 63–67.

VTT WORKING PAPERS

VTT RAKENNUS- JA YHDYSKUNTATEKNIIKKA –
VTT BYGG OCH TRANSPORT – VTT BUILDING AND TRANSPORT

4 Hietaniemi, Jukka, Hostikka, Simo & Vaari, Jukka. FDS simulation of fire spread – comparison of model results with experimental data. 2004. 46 p. + app. 6 p.

6 Viitanen, Hannu. Betonin ja siihen liittyvien materiaalien homehtumisen kriittiset olosuhteet – betonin homeenkesto. 2004. 25 s.

7 Gerlander, Riitta & Koivu, Tapio. Asiantuntijapalvelu yritysten innovaatiojohtamisen kehittämiseksi Piilaakson osaamiseen tukeutuen. IMIT SV -hankkeen loppuraportti. 2004. 25 s. + liitt. 11 s.

11 Lakka, Antti. Rakennustyömaan tuottavuus. 2004. 26 s. + liitt. 15 s.

14 Koivu, Tapio, Tukiainen, Sampo, Nummelin, Johanna, Atkin, Brian & Tainio, Risto. Institutional complexity affecting the outcomes of global projects. 2004. 59 p. + app. 2 p.

15 Rönty, Vesa, Keski-Rahkonen, Olavi & Hassinen, Jukka-Pekka. Reliability of sprinkler systems. Exploration and analysis of data from nuclear and non-nuclear installations. 2004. 89 p. + app. 9 p.

18 Nyyssönen, Teemu, Rajakko, Jaana & Keski-Rahkonen, Olavi. On the reliability of fire detection and alarm systems. Exploration and analysis of data from nuclear and non-nuclear installations. 2005. 62 p. + app. 6 p.

19 Tillander, Kati, Korhonen, Timo & Keski-Rahkonen, Olavi. Pelastustoimen määräiset seurantamittarit. 2005. 123 s. + liitt. 5 s.

20 Simo Hostikka & Johan Mangs. MASIFIRE – Map Based Simulation of Fires in Forest-Urban Interface. Reference and user's guide for version 1.0. 2005. 52 p. + app. 2 p.

21 Kortesmaa, Markku & Kevarinmäki, Ari. Massiivipuu maatilarakentamisessa. Suunnitteluohje. 2005. 76 s. + liitt. 6 s.

22 Ojanen, Tuomo & Ahonen, Jarkko. Moisture performance properties of exterior sheathing products made of spruce plywood or OSB. 2005. 52 p. + app. 12 p.

27 Kevarinmäki, Ari. Konenaulojen ulosvetolujuus. 2005. 24 s. + liitt. 12 s.

29 Oksanen, Tuuli, Kevarinmäki, Ari, Yli-Koski, Rainer & Kaitila, Olli. Ruostumattomasta teräksestä valmistettujen puurakenteiden liitosten palonkestävyys. 2005. 104 s. + liitt. 108 s.

31 Hietaniemi, Jukka. A Probabilistic Approach to Wood Charring Rate. 2005. 53 p.

32 Korhonen, Timo & Hietaniemi, Jukka. Fire Safety of Wooden Façades in Residential Suburb Multi-Storey Buildings. 2005. 66 p. + app. 40 p.

37 Hietaniemi, Jukka & Rinne, Tuomo. Tulipalojen yksittäispäästöt ilmaan: laskennallinen lähestymistapa. 2005. 78 s.

38 Kevarinmäki, Ari, Oksanen, Tuuli & Yli-Koski, Rainer. Ruostumattomasta teräksestä valmistettujen puurakenteiden liitosten suunnittelu. Yleiset ohjeet ja palomitoitus. 2005. 51 s. + liitt. 12 s.

39 Mroz, Arkadiusz & Kärnä, Tuomo. Mitigation of ice loading. Feasibility study of semi-active solution. 2005. 34 p.

ISBN 951–38–6591–6 (URL: http://www.vtt.fi/inf/pdf/)
ISSN 1459–7683 (URL: http://www.vtt.fi/inf/pdf/)